Biosensors and Bioelectronics 77 (2016) 90–98

Contents lists available at ScienceDirect

Biosensors and Bioelectronics

journal homepage: www.elsevier.com/locate/bios

# Development of double-generation gold nanoparticle chip-based dengue virus detection system combining fluorescence turn-on probes

Yen-Ting Tung [a], Cheng-Chung Chang [b,*], Yi-Ling Lin [c], Shie-Liang Hsieh [d,e], Gou-Jen Wang [a,b,*]

[a] Ph.D. Program in Tissue Engineering and Regenerative Medicine, National Chung-Hsing University, Taichung, Taiwan
[b] Graduate Institute of Biomedical Engineering, National Chung Hsing University, 250 Kuo Kuang Road, Taichung 402, Taiwan
[c] Institute of Biomedical Sciences, Academia Sinica, Taipei 115, Taiwan
[d] Genomics Research Center, Academia Sinica, Taipei 115, Taiwan
[e] Institute of Clinical Medicine, National Yang-Ming University, Taipei 112, Taiwan

ARTICLE INFO

*Article history:*
Received 26 July 2015
Received in revised form
2 September 2015
Accepted 3 September 2015
Available online 12 September 2015

*Keywords:*
DV (dengue virus)
CLEC5A receptor
Gold nanoparticle
Fluorescent turn-on probes
Fluorescence microscopy
Nanohemispheres

ABSTRACT

A sensing platform, combined amino acid labeling kit and a double-generation gold nanoparticle (DG-AuNP) chip, was designed to prove the existence of weak but crucial binding between the DV (dengue virus) and its CLEC5A receptor. At first, we have designed a kit combining the novel fluorescence turn-on sensors for lysine, arginine and cysteine amino acids. Advantages of this kit are that emission on–off switching can increase the signal-to-noise ratio and the virus must be fluorescently labelled with sufficient numbers of fluorophores because the lysine, arginine and cysteine residues of viral proteins are labelled simultaneously. Consequently, this kit can be used to light-on single DV spot both in solution and in cell under fluorescence microscopy. Second, the labeling kit was used to examine the DV binding to the CLEC5A-coated DG-AuNP chip. Based on our study, the double-generation gold nanoparticle construction of chip can support more coating areas for receptor CLEC5A and then, support more binding opportunities for DV. Meanwhile, the grooves between nanohemispheres will provide the extra driving force for DV stacking. We try to give a proof that this sensing platform is very useful for detection of weak binding mechanism.



## 1. Introduction

Dengue hemorrhagic fever (DHF), is caused by any of four dengue virus serotypes (serotype 1–4); is characterized by hemorrhagic manifestations, thrombocytopenia, and plasma leakage; and has the potential to further develop into dengue shock syndrome (DSS) with a 1–2.5% mortality rate (Back and Lundkvist, 2013; Yacoub et al., 2013). Characterizing the dengue virus (DV) recognition/entry receptors is crucial to illustrate the mechanism of DV pathogenesis to enable the specific treatment of DV infections by developing anti-DV drugs or vaccines. Both the mannose receptor (MR) and Dendritic Cell-Specific Intercellular adhesion molecule-3-Grabbing Nonintegrin (DC-SIGN) receptor have been reported to regulate DV binding and entry (Miller et al., 2008; Navarro-Sanchez et al., 2003; Tassaneetrithep et al., 2003). Furthermore, we showed that CLEC5A (C-type lectin domain family 5, member A) can interact directly with the dengue virion and act as a signaling receptor to stimulate the release of proinflammatory cytokines. That is, although the CLEC5A–DV interaction does not result in viral entry, it can mediate DV-induced proinflammatory cytokine production and pathogenesis (Chen et al., 2008). This major breakthrough in understanding the mechanism of DV pathogenesis may offer a promising strategy to alleviate tissue damage and increase the survival of patients suffering from DHF and dengue shock syndrome.

The interaction between CLEC5A and DV is very weak, although CLEC5A can also be identified by an Enzyme-linked immunosorbent assay (ELISA)-based innate immunity receptor array in the same way as the DV-specific receptors DC-SIGN and DC-SIGNR (Chen et al., 2008; Hsu et al., 2009). Thus, a more sensitive and reliable platform should be developed to overcome the challenge resulting from the weak binding between CLEC5A and DV, and would represent a good contribution to diagnostic developments. In previous work, we combined EIS (electrochemical impedance spectroscopy) and a nanostructured chip to develop an effective method to verify the weak conjunction between the

* Correspondence to: Graduate Institute of Biomedical Engineering, National Chung Hsing University, Taichung 402, Taiwan. Fax: +886 4 228 52422.
*E-mail address:* ccchang555@dragon.nchu.edu.tw (C.-C. Chang).

http://dx.doi.org/10.1016/j.bios.2015.09.007
0956-5663/

glycoprotein at the envelope of DV and CLEC5A (Tung et al., 2014). CLEC5A was immobilized on the gold nanoparticles deposited in a nanohemisphere array on the anodic aluminum oxide (AAO) surface to construct a DV-detecting biosensor chip. The bonding between CLEC5A and DV can be detected by the change in impedance before and after the immobilization of DV on a CLEC5A-coated electrode. In this case, the nanohemisphere array is necessary because no impedance difference was observed when the receptor was coated on a flat gold surface. We proposed that the defect sites (grooves) between nanohemispheres would provide the driving force for ligand binding. The main goal of the current manuscript is to visualize the location of DV on the CLEC5A-coated chip and prove that DV is located in the groove between the nanoparticles.

Fluorescence labeling is a popular and powerful method to visualize viruses, with direct chemical labeling with a small organic fluorescent dye as the most common general strategy. However, because of the small structure of viruses, viruses must be labeled with a sufficient number of fluorophores to enable detection without inhibiting their infectivity (Brandenburg and Zhuang, 2007; Sivaraman et al., 2011; Seisenberger et al., 2001). The DV labeling dyes DiD/DiI and Alexa Fluor 488/594 are known as membrane-fusion lipophilic dyes and amine reactive dyes, respectively (Ayala-Nuñez et al., 2011; Van der Schaar et al., 2007; Zhang et al., 2010). However, these dye molecules either cause a self-quenching effect at high labeling densities or only a limited number of fluorescent chemical labels can be attached to a virus particle (Wojta-Stremayr and Pickl, 2013). Therefore, a fluorescent emission enhancement protocol was designed to label viral proteins. In this study we have designed a kit combining the novel fluorescence turn-on sensors for lysine, arginine and cysteine amino acids. One advantage of this kit is that emission on–off switching can be used to negate the background signal problem and increase the signal-to-noise ratio. Furthermore, the virus must be fluorescently labelled with sufficient numbers of fluorophores because the lysine, arginine and cysteine residues of viral proteins are labelled simultaneously. Thus, this protocol enables the direct visualization of the DV actually binding on the CLEC5A-coated DG-AuNP chip, and we evaluate the diagnostic applications of the biochip. The experimental strategy and process are illustrated in Fig. 1.

## 2. Experiment

### 2.1. Materials and apparatus

The general chemicals employed in this study were of the best grade available and were obtained from Acros Organic Co., Merck Ltd., or Aldrich Chemical Co. and used without further purification. All solvents were of spectrometric grade. The sensing probes (CLEC5A, DC-SIGN) were constructed by Dr. Hsieh's lab, which contained a human IgG1 Fc region and lectin ligands as its Fab region (Chen et al., 2008). The FreeStyle 293 Expression System (Invitrogen) were used in overexpressed both sensing probes followed by purifying with protein A beads (GE Healthcare). Dengue virus (DV2/PL046) was kindly provided by Dr. Lin's lab according to Shih's method (Shih et al., 2004). The dengue virus was propagated in C6/36 cells. The viral titers were measured by plaque-forming-assays with BHK-21 cells.

Absorption spectra were generated using a Thermo$^{TM}$ Genesys$^{TM}$-6 UV–visible spectrophotometer, and fluorescence spectra were recorded using a HORIBA JOBIN-YVON Fluoromas-4 spectrofluorometer with a 1-nm band-pass in a 1-cm cell length at room temperature. The fluorescence images were taken under Leica AF6000 confocal fluorescence microscopy with DFC310 FX Digital color camera. Atomic force microscopy (AFM) measurements were performed under a liquid environment (with a liquid

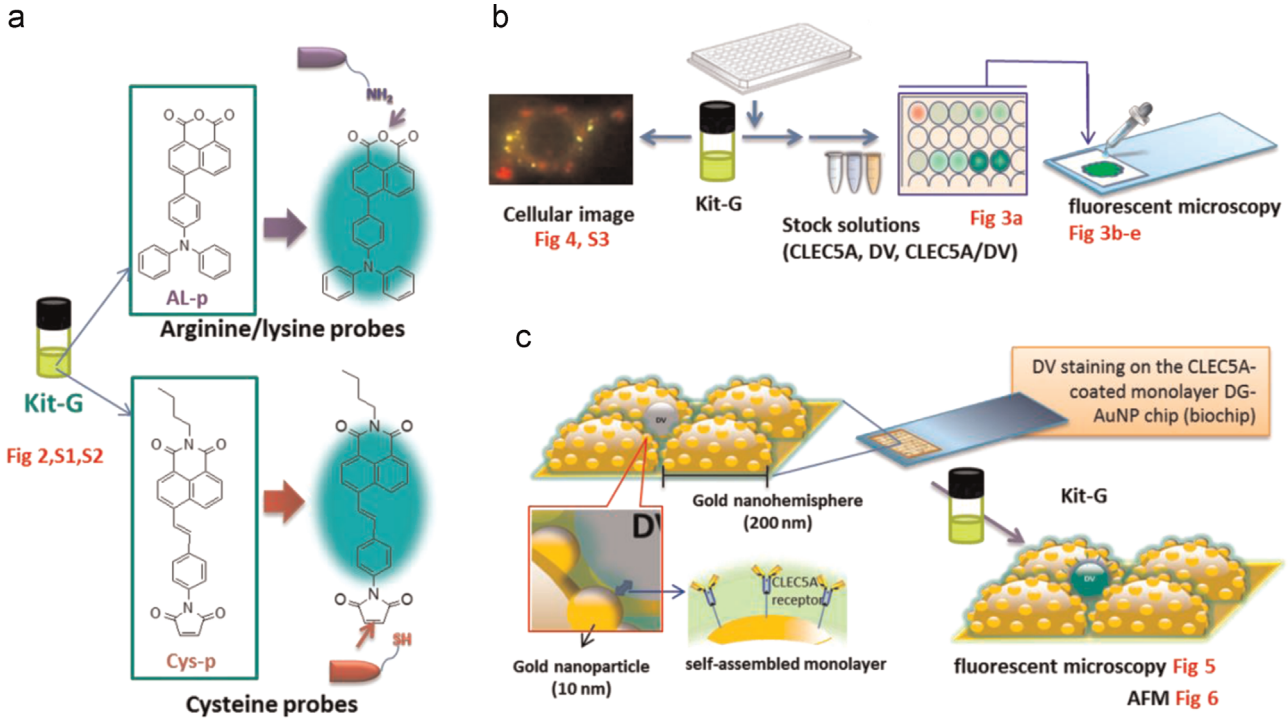


**Fig. 1.** (a) The proposed fluorescence turn-on mechanisms of the designed arginine/lysine probe (up) and cysteine-probe (down) and the components of kit-G (emission turn-onto a bright green color). (b, c) Illustration of the molecular imaging strategy. (b) Fluorescent labeling of the receptor and virus using kit. (c) The construction of a double-generation gold nanoparticle (DG-AuNP) chip and the fluorescent labeling of this chip using kit. In this case, the virus is bound to the receptor-coated Au surface. (For interpretation of the references to color in this figure legend, the reader is referred to the web version of this article.)

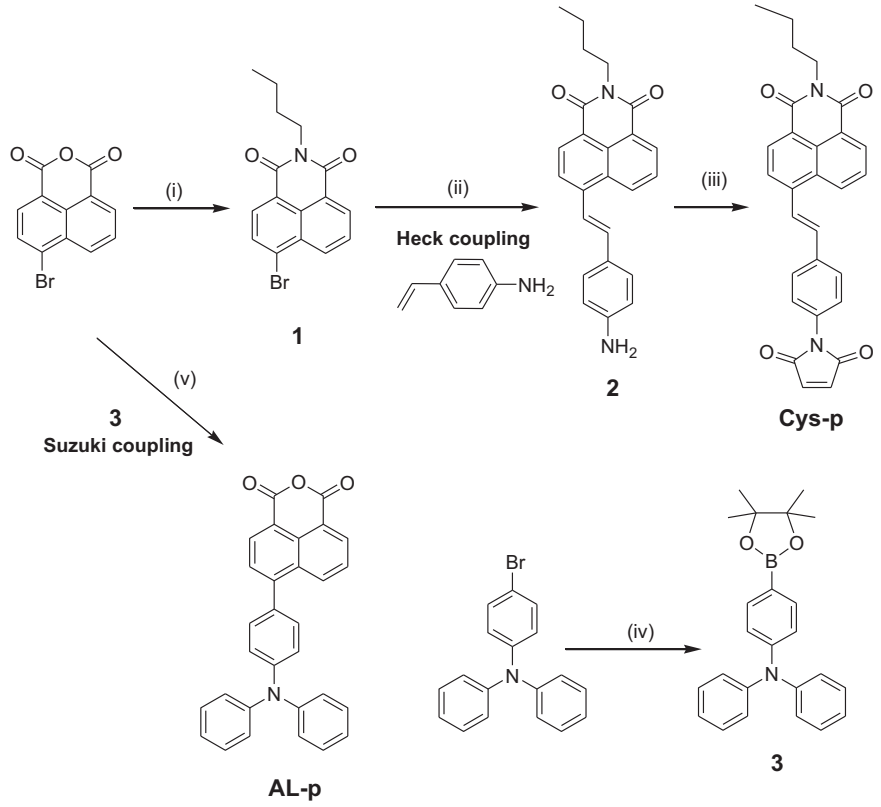


**Scheme 1.** Reagents and conditions: (i) N-butylamine, EtOH, r.t. 24 h; (ii) $Pd(OAc)_2/(o\text{-}tol)_3P$, 4-aminostyrene, $MeCN/Et_3N$, $N_2$, reflux 48 h; (iii) (a) maleic anhydride, $CHCl_3$, reflux 24 h, (b) sodium acetate, acetic anhydride, 90–100 °C 24 h; (iv) pinacolborane, $Pd(PPh)_3Cl_2$, $dioxane/Et_3N$, $N_2$, reflux 12 h; (v) $K_2CO_3$, $Pd(OAc)_2/(o\text{-}tol)_3P$, compound **3**, $DME/H_2O$, $N_2$, reflux 48 h.

cell) via Dimension-icon AFM (Bruker Instruments). In this mode, probe is operated in a 2 kHz oscillation, amplitude is 100 nm, and scanning rate is 0.8 Hz. Consider the scale of virus; the scanning range and resolution are set to 2.5 μm × 2.5 μm and 256 × 256 lines, respectively. The used AFM probe is AppNano silicon nitride cantilever (Nitra-All series) with the spring constant between 0.04 and 0.32 (N/m), which suits the imaging of soft or delicate sample in liquid phase. The AFM probes were attached on a fluid cantilever (DECAFMCH-DD) and immersed in BSA.

## 2.2. Methods

### 2.2.1. Fabrication of a double-generation gold nanoparticle (DG-AuNP) chip

The composition of the nanostructured sensor chip was described in our previous study (Tsai et al., 2011). The fabrication of the proposed 3-D nanostructured biosensor includes: AAO film preparation, barrier layer surface modification, Au thin film deposition, electrode annealing, device packing, and Au nanoparticle deposition. Refer the scanning electron microscope (SEM) image, the Au deposited AAO barrier layer of uniformly distributed nanohemispheres with a diameter about 200 nm and gold nanoparticle were uniformly and compactly deposited on the orderly hemispheric electrode array with an average diameter of less than 10 nm. The device about Au nanoparticle deposition on gold nanohemispheres surface is named a DG-AuNP (double-generation gold nanoparticle) chip and its schematic diagram is shown in Fig. 1b.

### 2.2.2. Immobilization of sensing probe on DG-AuNP chip to become biochip

The self-assembled monolayer (SAM) process was applied to immobilize the sensing probes onto the sensor surface. First, we treated the electrode surface with 20 μL, 10 mM 11-mercaptoundecanoic acid solution for 10 min, followed by interaction with a 20 μL mixed solution of 50 mM N-hydroxysuccinimide and 100 mM 1-ethyl-3-(3-dimethylamino propyl)-carbodiimide. Then, we incubated it with the probes (CLEC5A and DC-SIGN) for 30 min (15 μL, the concentration of the implemented probes was 0.02 μg/μL for hIgG1and 0.012 μg/μL for the other probes). The sensor chips were then blocked with the culture medium for 45 min, after which the sensor chip was incubated with DV (DV titer is $9.5 \times 10^7$ plaque forming units/mL; pfu/ mL) for another 30 min (Fig. 1b).

### 2.2.3. Kits labeling of virus-bound biochip

The DG-AuNP chips were coated with receptors (such as CLEC5A) to become biochips; then they were incubated with kit-G (10 μM) for 5–7 min, followed by gentle destaining with ethanol three times before the imaging study.

### 2.2.4. Conjugated fluorescent-antibody assay

Baby hamster kidney BHK-21 cells were prepared with a number of $1 \times 10^4$/96-well plates. Cells were adsorbed with DENV-2 for 2 h at 4 °C with rocking on a linear shaker. After incubation, cells were washed with cold PBS and fixed with 4% paraform-aldehyde for 1 h at room temperature. For immuno-staining, cells were treated with 4% paraformaldehyde followed by block with protein free blocking buffer at room temperature for 1 h. The cells were stained with anti-E antibody followed by Alexa Fluor 568-conjugated secondary antibody (anti-M IgG568). Antibody amplification scheme using our superior Alexa Fluor® conjugates, permitting enhanced detection of mouse primary antibodies. The Alexa Fluor® Signal Amplification Kits for mouse antibodies containing antibody conjugates of the Alexa Fluor® 568 (Cat. no. A11066) dyes, which yield red–orange fluorescence. An Alexa

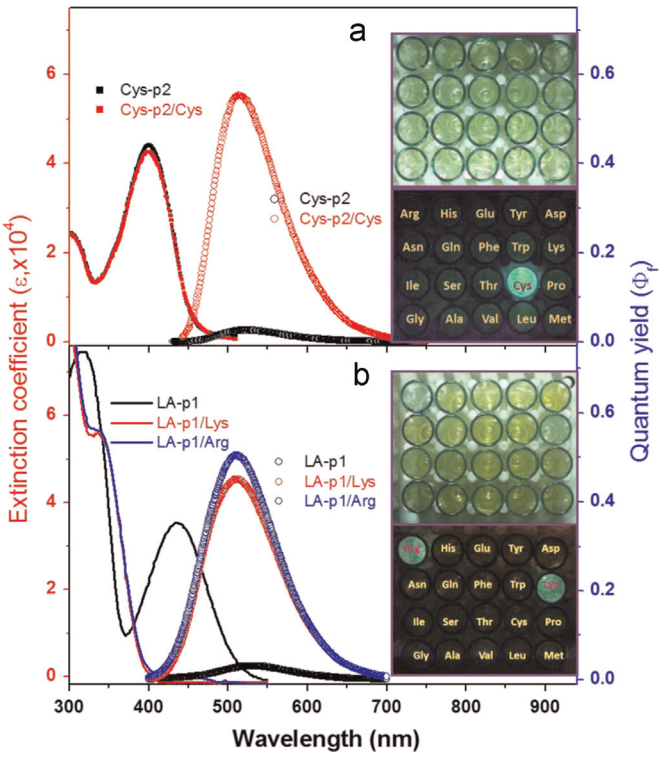


**Fig. 2.** (a) Cysteine-induced absorption (left) and fluorescence (right, $\lambda_{ex}$=400 nm) of Cys-p and (b) arginine/lysine-induced absorption (left) and fluorescence (right, $\lambda_{ex}$=340 nm) of AL-p in ethanol represented by extinction coefficient and quantum yield, respectively. The inset photos show the emission color changes of the probes (10 μM) in the presence of all 20 amino acids (10 eq.) under a handheld ultraviolet lamp (365 nm). (For interpretation of the references to color in this figure, the reader is referred to the web version of this article.)

Fluor® rabbit anti-mouse IgG antibody conjugate is used to bind to the mouse primary antibody.

*2.2.5. General procedure for the synthesis of cysteine probes (naphthalimide derivatives) and lysine/arginine probes (1,8-naphthalic anhydride derivatives)*

As depicted in Scheme 1, synthesis of the naphthalimide derivatives: the first stage of the reaction, in which commercial starting material 4-bromo-1,8-naphthalic anhydride was reacted with the N-butylamine, was performed conveniently in ethanol under room temperature. Next, the samples were subjected to the Heck coupling reaction. Synthesis of the 1,8-naphthalic anhydride derivatives: we used N-(4-bromophenyl)-N-phenyl-benzenamine to prepare intermedium **3** which were subjected to the Suzuki coupling reaction with 4-bromo-1,8-naphthalic anhydride, respectively. Details of materials synthetic procedures and identifications are shown in the Supporting information.

## 3. Result and discussion

### *3.1. Molecular design and synthesis*

Multiple fluorescent probes such as chemical labels (amino-reactive dyes, lipophilic dyes, metabolic labels, etc.) and fluorescent proteins can be used to visualize individual virus particles. We have designed and synthesized fluorescence turn-on sensors to label the amino acids lysine, arginine and cysteine of viral proteins, respectively. Michael addition reactions and maleimide conjugation of fluorophores have been widely used in the development of chemical probes for thiols, and have been applied in a wide variety of studies. Many probes bearing a maleimide group have been reported as fluorescent labels for thiols (Matsumoto et al., 2007; Guo et al., 2009; Liu et al., 2010; Kand et al., 2012). These probes react rapidly with thiols and are used to fluorescently label proteins. On the other hand, the detection or quantification of lysine has been applied in studies of cell biology, disease, foods and plants (Chalova et al., 2008; Ansari and Moinuddin, 2011; Ciriello et al., 2015; Chen et al., 2010) Moreover, selective recognition of arginine (Arg) is vital as it forms the immediate precursor of NO, urea, ornithine and agmatine; it also plays an important role in cell division, immune function and hormone release (Stechmiller et al., 2005). However, because of their hydrophilic character and the weak interactions between sensors and amino acids, a limited number of studies have reported fluorescent sensors to recognize arginine (Pu et al., 2013; Pirkle and Pochapsky, 1987; Zhou et al., 2011) and lysine (Minami et al., 2014; Wehner et al., 2000; Rawat and Kailasa, 2014). Furthermore, unlike N-terminal protein labeling reactions, using fluorescence turn-on organic molecules to conjugate amine-side-chain containing amino acids is a rare application.

In previous studies, we have described the unique fluorescent properties of naphthalimide derivatives (Lin et al., 2011). In particular, we found that 4-bromo-1,8-naphthalic anhydride can easily conjugate with primary amines in the presence of ethanol system. Thus, two fluorescence turn-on fluorophores with visible-wavelength emissions were designed. Cysteine probes were prepared by conjugating a maleimide to naphthalimide fluorophores. The starting material N-butyl-4-bromo-1,8-naphthalimide, was converted to the intermediate N-butyl-4-(aminophenyl)-1.8-naphthalimide and then to N-butyl-4-(4-aminostyryl)-1.8-naphthalimide, and the target compounds Cys-p was obtained by means of Heck reactions. The arginine/lysine probes retained the 1,8-naphthalic anhydride functional group, and the target compounds AL-p was obtained directly by means of Suzuki reactions (Scheme 1). Here, we have designed and synthesized fluorescence turn-on sensors to label the amino acids lysine, arginine and cysteine of viral proteins, respectively.

### *3.2. Spectral investigation of amino acid probes*

The basic and cysteine-induced absorption and fluorescence spectral properties of the cysteine probes are shown in Fig. 2a. Upon the addition of cysteine (10 eq.) to the probe-containing ethanol solution, the absorbance patterns of Cys-p did not exhibit any apparent change. At the same time, the emission intensities increased with quantum yields increasing from ~0.021 (522 nm) to 0.57 (515 nm). The quantum yields were determined by referring to a reference (Lin et al., 2011). The fluorescence responses of Cys-probe to various amino acids were also investigated. The inset photos in Fig. 2a show that no obvious changes in this probe was observed upon the addition of other natural amino acids. Both the relative selectivity spectrum and the titration spectrum indicate that probe Cys-p displayed high selectivity and sensitivity for cysteine (Fig. S1).

Fig. 2b shows the spectral variations upon the addition of arginine and lysine to the probe. In ethanol system, the absorption bands of AL-p centered at 430 nm decreased and new bands centered at 340 nm appeared, with an apparent emission enhancement from a quantum yield of ~0.029 (530 nm) to 0.53 (515 nm, Arg) and 0.48 (512 nm, Lys). Here, similar spectral changes, hypochromic shifts in absorption and intensity increases in emission spectra were observed when 10 eq. of arginine and lysine were added to each of the probe-containing ethanol solutions. The fluorescence responses of AL-probes to 20 amino acids were also investigated. No significant variation in fluorescence intensity was found in comparison with experiments containing

only Lys or Arg. Importantly, the structurally related amino acids asparagine (Asn) and glutamine (Gln) exhibited low reactivity to the probes, which may be due to their amide resonance. Meanwhile, tryptophan (Trp), histidine (His), proline (Pro) and other amine acids hardly reacted with the probes under these conditions. The arginine/lysine-relative selectivity and sensitivity spectra of AL-p were also presented in the Supporting Information (Fig. S2). To the best of our knowledge, this is the first report about arginine/lysine probes based on carboxylic anhydride group. Based on the results in Fig. 2, we prepared a $10^{-2}$ M Cys-p and AL-p mixed stock solution, which exhibited a fluorescent emission turn-onto a bright green color when reacting with the appropriate amino acids, referred to as labeling kit-G. These stock solutions are diluted to $10^{-5}$ M with ethanol for actual use. The proposed fluorescence turn-on mechanism of the designed amino acid probes and the kit components are shown as in Fig. 1a. We expect that both kits can simultaneously label the cysteine, arginine and lysine residues of the virus.

### 3.3. Fluorescence turn-on labeling of virus in solution and in cell

We next applied the labeling kit to label CLEC5A, blocking protein and DV. First, the kit stock solution was added to the wells of the plate to prepare 10 μM probe-containing buffer and ethanol solutions, respectively. Then, every test analyte (20 μL, 100$\lambda$) was added to each well individually. Fig. 3a shows that our novel kits can easily label the proteins of these analytes and become bright due to emission enhancement in ethanol. More important, the probe-bound DV could be visualized using 365 nm UV light from handheld UV lamps. With respect to the control wells, detection with brilliant green colors can be achieved with kit-G. Based on our hypothesis, we expected that fluorophore binding to DV would result in sufficiently bright emission to observe individual DV particles under fluorescence microscopy. We want to claim that once these three mentioned amino acids are included in viral protein of other virus, it is very possible that our kit can also label these viruses and the fluorescence turn-on efficiency should depend on the quantities of these three mentioned amino acids. We believe that the recognition of variable viruses is very important issue. Nevertheless, herein the resulting ethanol solutions in Fig. 3a were further investigated using fluorescence microscopy.

Fig. 3d and e clearly depict bright spots, which present the labeling DV could be imaged by fluorescence microscopy in the A cube fluorescence channel (using a 370 ± 10 nm band pass filter as the excitation light source, with emission collected through a 450 nm long pass filter). As controls, though CLEC5A and blocker-protein containing solutions (Fig. 3b and c) showed green fluorescence turn-on background due to the reactive amino acid labeled by kit, there were no green spots could be observed in the micrographs even using longer timer-exposure condition. This

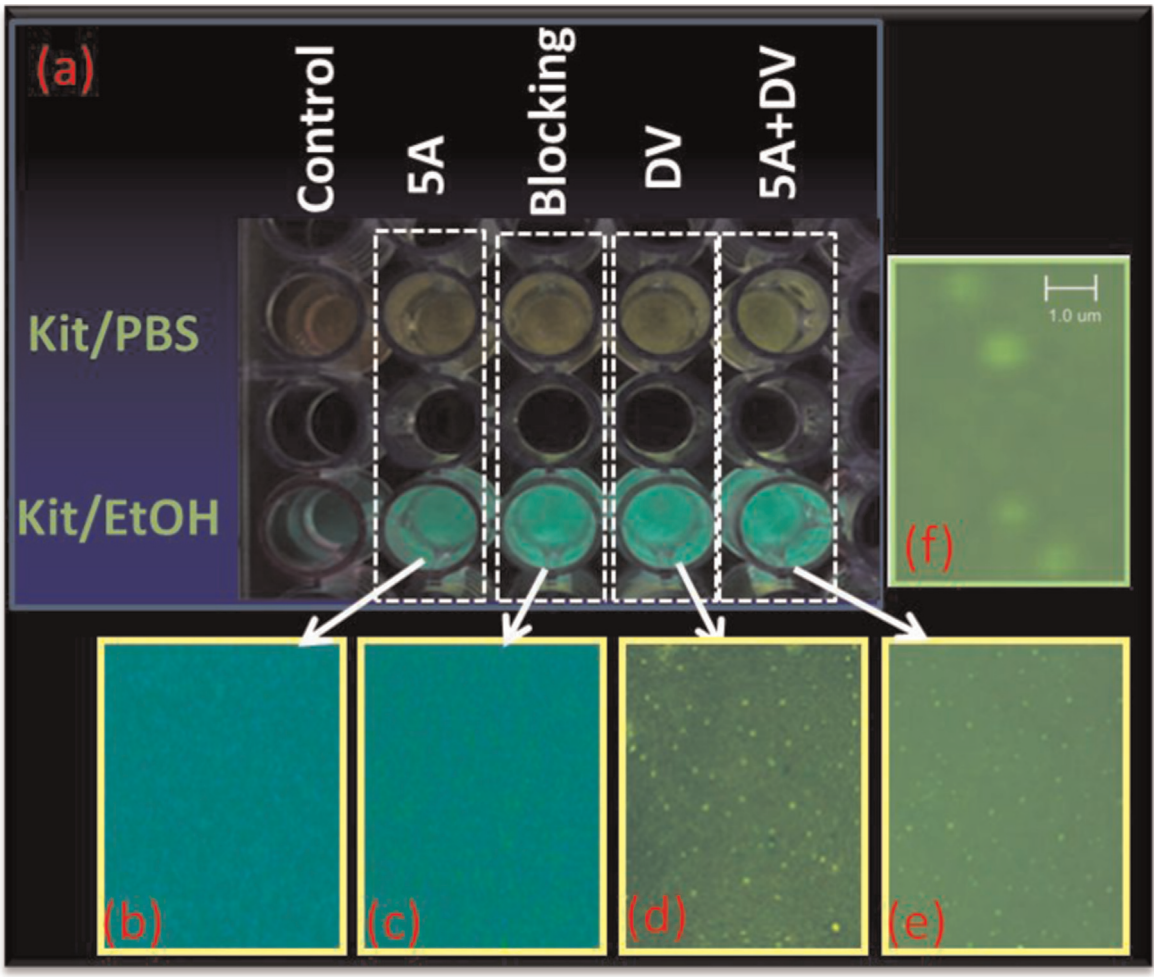


**Fig. 3.** Fluorescence turn-on labeling of virus using the kit-G. (a) The color changes, exciting from 365 nm handheld UV lamps, of 10 μM kit-G in PBS (up) and ethanol (down) in the absence and presence of CLEC5A, blocking protein, DV and CLEC5A+DV (from left to right). (b)–(e) A fluorescent microscopic image of kit-G labeled CLEC5A, blocking protein, DV and CLEC5A+DV (from left to right) in ethanol with the A cube channel (a 370 ± 10 nm band pass filter as the excitation light source, with emission collected through a 450 nm long pass filter). (f) A zoomed-in view of the spots; the scale bars in the figures represent 1 μm. (For interpretation of the references to color in this figure legend, the reader is referred to the web version of this article.)

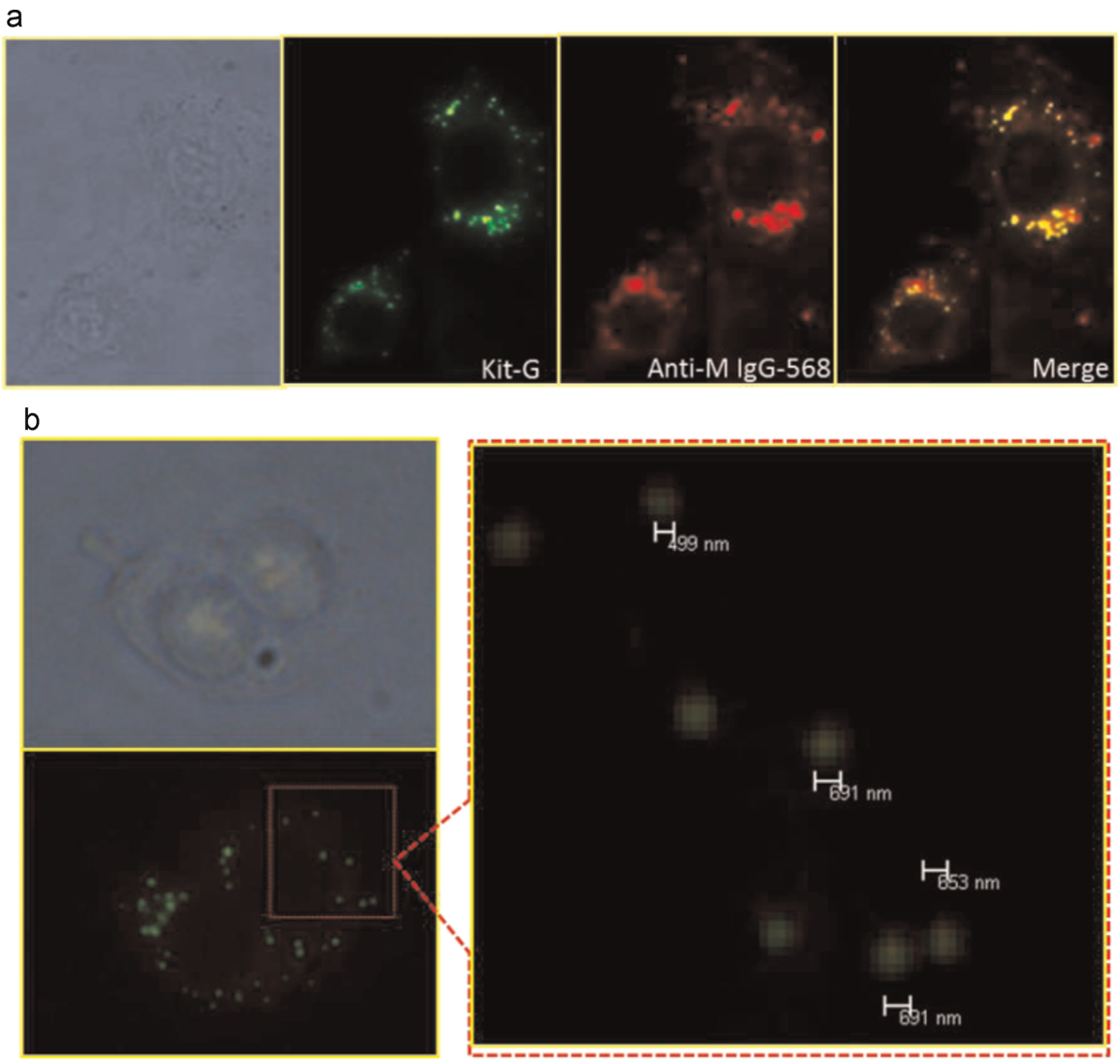


**Fig. 4.** (a) Co-localization assay of fixed DV-infected BHK-21 cells which were pre-stained with fluorophore-labeling antibody anti-M IgG-568 first and then attained with kit-G (4 min). From left to right: bright-field, stained with kit-G, stained with anti-M IgG-568 and merge of green and red images. The green image of kit-G was excited by a A cube channel (a 370 ± 10 nm band pass filter as the excitation light source, with emission collected through a 450 nm long pass filter); red image of anti-M IgG-568 was excited by a N cube channel (a 535 ± 25 nm band pass filter as the excitation light source, with emission collected through a 590 nm long pass filter). (b) Bright spots and its zoom in image of BHK-21 cells infected with kit-G labeling-DV. (For interpretation of the references to color in this figure legend, the reader is referred to the web version of this article.)

result confirmed that our kit can be used to label DV and that these labeled DVs were bright enough to be observed under fluorescence microscopy. This is a very important result supporting our strategy for DV detection because it represents the basis of the experiment depicted in Fig. 1b; we wanted to image DV on the chip stained with these two kits to emphasize the virus-receptor binding that occurs between the chip and DV.

More than two hundred spots were collected and measured from Fig. 3. It is estimated that these observable bright spots are between 600 nm and 800 nm scales, as shown in Fig. 3f, larger than actual DV size (~50 nm, see the discussion of next section from AFM result) due to the emission halation of labeled DVs. Namely, the bright spots we observed were single fluorescence-virus spots but were not single virus. This approach was further confirmed by conjugated fluorescent-antibody assay, as Fig. 4a shows. When we stained the kit-G to the fixed DV-infected baby hamster kidney BHK-21 cells, which were pre-stained with fluorophore-labeling antibody anti-M IgG-568, the fluorescent spots from kits merged well with the red fluorescent spots of fluorophore-labeling antibody. Meanwhile, Fig. 4b reveals clear spots in the cellular images of kit-G-labeling DV infected BHK-21 cells. We also collected the similar size (600~800 nm) fluorescent spots from these virus-infected cells and their shapes and sizes were similar to the results in Fig. 3. Consequently, similar result in Fig. 4a was observed when stained these kit-G labeling-DV infected BHK-21 cells with fluorophore-labeling antibody anti-M IgG-568 (Fig. S3). Additionally, compare with the shapes and sizes of the fluorescent spots of fluorophore labeling-DV (or virus) from other literature reports (Ayala-Nuñez et al., 2011; Balogh et al., 2011; Brandenburg and Zhuang, 2007; Cui et al., 2011; Van der Schaar et al., 2007). It is reasonable to assume that these bright spots represent individual DV particles. That is, a novel fluorescence turn-on single virus sensor kit-G was developed successfully. The advantage of this kit is low background signal and high signal-to-noise ratio. Furthermore, the virus must be fluorescently labelled with sufficient numbers of fluorophores because the lysine, arginine and cysteine residues of viral proteins are labelled simultaneously in a very short time.

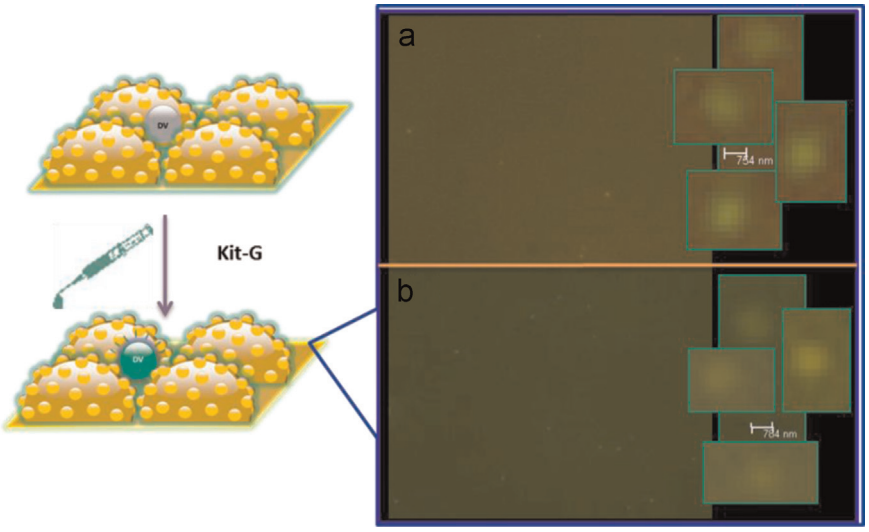


**Fig. 5.** Fluorescence turn-on labeling of virus-bound biochip using the labeling kit-G. Fluorescent microscopic images of (a) DV binding to a CLEC5A-coated DG-AuNP chip stained with kit-G and observed under the A cube channe. (b) DV binding to a DC-SIGN-coated DG-AuNP chip stained with kit-G and observed under the A cube channel. The insets show the zoomed-in views of the spots and their size scales estimation.

### 3.4. Fluorescence turn-on labeling of virus-bound biochip

After testing various staining conditions, we selected the optimal procedure as described in Section 2 and Fig. 1c to collect reproducible DV-imaging on chip under fluorescence microscopy. Fig. 5a shows the fluorescent spots produced by staining with kit-G. Again, the fluorophore-labeled DV could be imaged on the chip using A cube channels. Meanwhile, to confirm that these signals are nanoscale DVs, Fig. 5b presents the control staining experiment to a DV-bound chip but coating with the DC-SIGN receptor instead of CLEC5A. More spots of a similar size are observed compared with Fig. 5a, from which we infer that more DV particles are present on the DC-SIGN-coated chip. This observation is consistent with previous studies concluding that the binding force between DV and CLEC5A is lower than that between DV and DC-SIGN. Furthermore, these DV-binding biochips were destained several times before observation, which is why few spots were observed. In this case we also collected more one hundred spots and got similar size scales as above results. Nevertheless, the key finding is that these fluorescence microscopic images enable direct observation of DV binding to the CLEC5A-coated DG-AuNP chip. We are able to collect reproducible images as shown in Fig. 5 by following the procedure described in the experimental section and believe that there is a single DV particle which binding on the biochip.

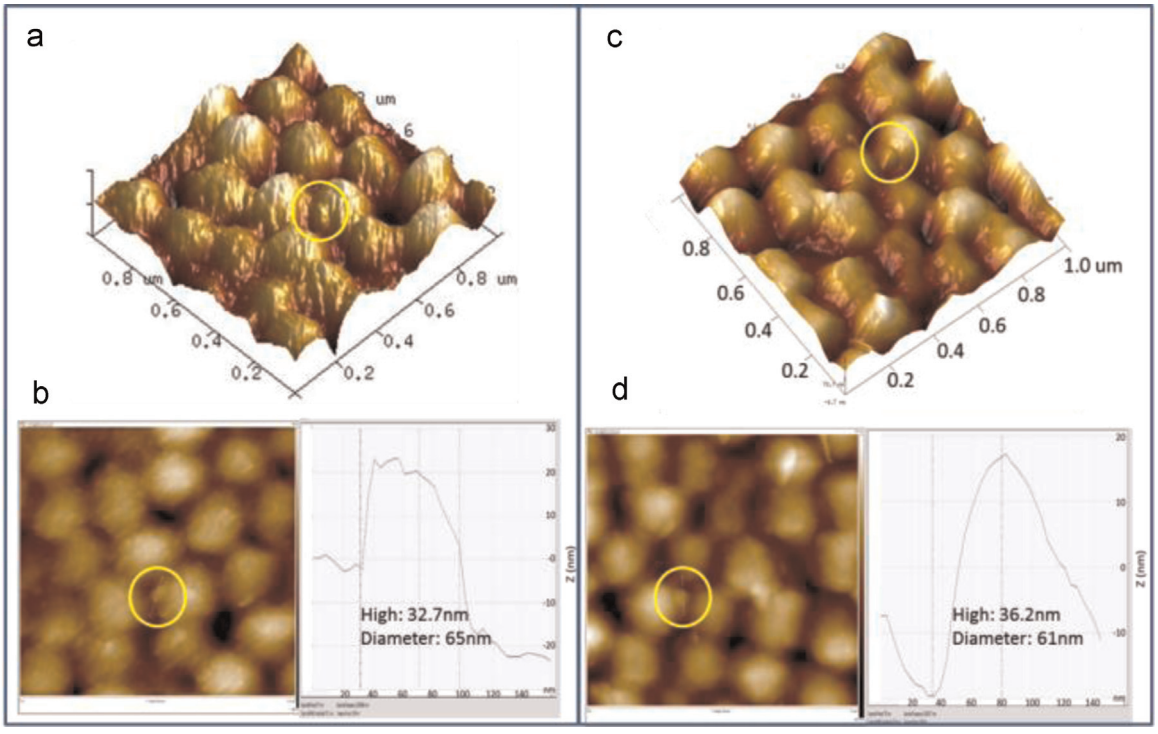


**Fig. 6.** AFM characterization of located DV on the biochip. Topographic images of DV incubated (a) CLEC5A-coated and (c) DC-SIGN-coated DG-AuNP chips and corresponding line scans (b, d). The scanning area is 1 μm × 1 μm.

### 3.5. The location of DV on the biochip characterized by AFM

The virus morphology under biological conditions can be determined by atomic force microscopy (AFM) in liquid phase. The virus was bound to the surface of a gold coated AAO to prevent the virus from moving freely and disturbing the AFM tip. The virus was attached to the surface by chemical modification of the functional group on the Au. This measurement was carried out by a Dimension-icon AFM (Bruker Instruments) in scanning mode, in which the sample surface is scanned by tapping using a constant peak force. This means that the force of the tip can be controlled to reduce the disturbance to the sample. Therefore, we decrease the force as much as possible while still capturing an image of sufficient quality. The AFM topographic image and line scans obtained for the DV-binding on the CLEC5A-coated biochip confirmed the previous data. Tapping mode AFM was used to check the integrity and location of the DV. As presented in Fig. 6a, the AFM image demonstrates smaller spherical particles in the gaps between nanohemispheres on the DG-AuNP chip. For comparison, images of DV incubated on a DC-SIGN coated biochip are presented in Fig. 6c, with similar results. The dimensions of the system measured using AFM are also presented. The AFM images and topographic profiles show a spherical particle with a diameter of 65 nm and a height of 32.7 nm in the CLEC5A system, as shown in Fig. 6b; and 65 and 36.2 nm in the DC-SIGN system, as shown in Fig. 6d. The particle sizes determined from this result are similar to the previous AFM data obtained by other groups (Ferreira et al., 2008; Pereira et al., 2010; Valenga et al., 2012), indicating that these particles represent mature spherical DV located in the grooves between gold nanohemispheres.

As Fig. 1c shows, the DG-AuNP chip enables the capture of DV particles onto the cavity formed by staggered arrangement hemispheres. Furthermore, each orderly distributed Au nanoparticle on the hemisphere surfaces that formed a cavity may facilitate the binding of a CLEC5A receptor onto it. Thereby, multivalent interactions between CLEC5A receptors and the DV particle that falls into a cavity can be enhanced. That is why the DG-AuNP chip, a novel virus detection platform, is an effective tool for studying the weak binding between a virus and its corresponding receptors. The main issue of this manuscript is to visualize and prove the binding model of this platform by taking advantage of fluorescence turn-on sensors. Therefore, a fluorescent emission enhancement protocol was designed to label viral proteins. The maleimide functional groups of Cys-p1 and Cys-p2 molecules can conjugate with thiols to become cysteine probes; the 1,8-naphthalic anhydride functional groups of AL-p1 and AL-p2 molecules can conjugate with primary amine to become arginine/lysine probes. Follow the experimental results, these fluorescence turn-on sensors can label the relative targeting amino acids with high sensitivity and selectivity. More important, prior to binding target amino acid, these probes exhibit low fluorescence. Hence, we expect that the probes-containing kit is emission on–off switchable which can be used to negate the background signal problem and increase the signal-to-noise ratio. However, consider the colorful background in these micrographs (Figs. 4b–e and 5), these signals should be the results of kits binding to proteins of CLEC5A receptors and/or blocking reagents, but they are not nano-structure spots. Nevertheless, the key finding is that the bright spots appear at the surface ends of the chip. That is, the fluorescence microscopy image provides direct observation and evidence of that DV binding on the CLEC5A-coated Chip. Although, within a photo image, not many spot signals were observed due to the weak binding between CLEC5A and DV, we were able to collect reproducible images.

## 4. Conclusion

In conclusion, this study reports the design of a combination method to investigate the binding between DV and its crucial receptor CLEC5A. We developed a kit containing lysine, arginine and cysteine targeting fluorescence turn-on probes, which can easily label appropriate amino acids of dengue virus (DV) proteins and light-on single DV spot both in solution and in cell under fluorescence microscopy. Combine a double-generation gold nanoparticle (DG-AuNP) biochip, the labeling kit was used to prove the existence of weak but crucial binding between the DV and the CLEC5A receptor and provide a proof that this platform is very useful for detection of weak binding mechanism.

## Acknowledgments

This work was supported financially by the National Science Council (NSC 101-2113-M-005 -016-MY3) and MOST (103-2321-B-001-070) of Taiwan. We also thank Dr. Mon-Shu Ho for assistance with the AFM measurements.

## Appendix A. Supplementary information

Supplementary data associated with this article can be found in the online version at http://dx.doi.org/10.1016/j.bios.2015.09.007.

## Reference

Ayala-Nuñez, N.V., Wilschut, J., Smit, J.M., 2011. Methods 55, 137–143.
Ansari, N.A., Moinuddin, Ali R., 2011. Dis. Markers 30, 317–324.
Back, A.T., Lundkvist, A., 2013. Infect. Ecol. Epidemiol 3, 18939–18960.
Balogh, A., Pap, M., Markó, L., Koloszár, I., Csatáry, L.K., Szeberényi, J., 2011. Enzyme. Microb. Technol 49, 255–259.
Brandenburg, B., Zhuang, X., 2007. Nat. Rev. Microbiol. 5, 197–208.
Chen, S.T., Lin, Y.L., Huang, M.T., Wu, M.F., Cheng, S.C., Lei, H.Y., et al., 2008. Nature 453, 672–676.
Chalova, V.I., Zabala-Diaz, I.B., Woodward, C.L., Ricke, S.C., 2008. World J. Microbiol. Biotechnol. 24, 353–359.
Ciriello, R., Cataldi, T.R., Crispo, F., Guerrieri, A., 2015. Food Chem. 169, 13–19.
Chen, I.C., Thiruvengadam, V., Lin, W.D., Chang, H.H., Hsu, W.H., 2010. Plant. Mol. Biol. 72, 153–169.
Cui, Z.Q., Ren, Q., Wei, H.P., Chen, Z., Deng, J.Y., Zhang, Z.P., Zhang, X.E., 2011. Nanoscale 3, 2454–2457.
Ferreira, G.P., Trindade, G.S., Vilela, J.M., Da Silva, M.I., Andrade, M.S., Kroon, E.G., 2008. J. Microsc. 231, 180–185.
Guo, X.F., Wang, H., Guo, Y.H., Zhang, H.S., 2009. Anal. Chim. Acta 633, 71–75.
Hsu, T.L., Cheng, S.C., Yang, W.B., Chin, S.W., Chen, B.H., Huang, M.T., et al., 2009. J. Biol. Chem. 284, 34479–34489.
Kand, D., Kalle, A.M., Varma, S.J., Talukdar, P., 2012. Chem. Commun. 48, 2722–2724.
Liu, Y., Yu, Y., Lam, J.W., Hong, Y., Faisal, M., Yuan, W.Z., Tang, B.Z., 2010. Chemistry 26, 8433–8438.
Lin, H.H., Chan, Y.C., Chen, J.W., Chang, C.C., 2011. J. Mater. Chem. 21, 3170–3177.
Miller, J.L., de Wet, B.J., Martinez-Pomares, L., Radcliffe, C.M., Dwek, R.A., Rudd, P.M., et al., 2008. PLoS Pathog. 4, e17.
Matsumoto, T., Urano, Y., Shoda, T., Kojima, H., Nagano, T., 2007. Org. Lett. 9, 3375–3377.
Minami, T., Esipenko, N.A., Zhang, B., Isaacs, L., Anzenbacher Jr., P., 2014. Chem. Commun. 50, 61–63.
Navarro-Sanchez, E., Altmeyer, R., Amara, A., Schwartz, O., Fieschi, F., Virelizier, J.L., et al., 2003. EMBO Rep. 4, 723–728.
Pu, W., Zhao, H., Huang, C., Wu, L., Xu, D., 2013. Anal. Chim. Acta 764, 78–83.
Pirkle, W.H., Pochapsky, T.C., 1987. J. Am. Chem. Soc. 109, 5975–5982.
Pereira, E.M., Dario, A.F., França, R.F., Fonseca, B.A., Petri, D.F., 2010. ACS Appl. Mater. Interfaces 2, 2602–2610.
Rawat, K.A., Kailasa, S.K., 2014. Microchim. Acta 181, 1917–1929.
Sivaraman, D., Biswas, P., Cella, L.N., Yates, M.V., Chen, W., 2011. Trends. Biotechnol. 29, 307–313.
Seisenberger, G., Ried, M.U., Endress, T., Büning, H., Hallek, M., Bräuchle, C., 2001. Science 294, 1929–1932.
Stechmiller, J.K., Childress, B., Cowan, L., 2005. Nutr. Clin. Pract. 20, 52–61.
Shih, S.R., Tsai, M.C., Tseng, S.N., Won, K.F., Shia, K.S., Li, W.T., et al., 2004. Antimicrob. Agents Chemother. 48, 3523–3529.
Tassaneetrithep, B., Burgess, T.H., Granelli-Piperno, A., Trump-fheller, C., Finke, J.,

Sun, S.L., et al., 2003. J. Exp. Med. 197, 823–829.
Tung, Y.T., Wu, M.F., Wang, G.J., Hsieh, S.L., 2014. Nanomedicine 10, 1335–1341.
Tsai, J.J., Bau, I.J., Chen, H.T., Lin, Y.T., Wang, G.J., 2011. Int. J. Nanomet. 6, 1201–1208.
Van der Schaar, H.M., Rust, M.J., Waarts, B.L., van der Ende-Metselaar, H., Kuhn, R.J., Wilschut, J., Zhuang, X., Smit, J.M., 2007. J. Virol. 81, 12019–12028.
Valenga, F., Petri, D.F., Lucyszyn, N., Jó, T.A., Sierakowski, M.R., 2012. Int. J. Biol. Macromol. 50, 88–94.
Wojta-Stremayr, D., Pickl, W.F., 2013. Sensors (Basel) 13, 8722–8749.
Wehner, M., Schrader, T., Finocchiaro, P., Failla, S., Consiglio, G., 2000. Org. Lett. 2, 605–608.
Yacoub, S., Mongkolsapaya, J., Screaton, G., 2013. Curr. Opin. Infect. Dis. 26, 284–289.
Zhang, S.L., Tan, H.C., Hanson, B.J., Ooi, E.E., 2010. J. Virol. Methods 167, 172–177.
Zhou, X., Jin, X., Li, D., Wu, X., 2011. Chem. Commun. 47, 3921–3923.